September, 1980] © *1980 The Chemical Society of Japan* *Bull. Chem. Soc. Jpn.*, **53**, *2535—2539 (1980)* 2535

Spin-state Equilibria of the Nickel(II) Complexes of 2,12-Dimethyl-3,7,11,17-tetraazabicyclo[11.3.1]heptadeca-1(17),2,11,13,15-pentaene Analogs in Water

Katsura Mochizuki, Masatoshi Fujimoto,* Haruko Ito,† and Tasuku Ito†
Department of Chemistry, Faculty of Science, Hokkaido University, Sapporo 060
† *Institute for Molecular Science, Okazaki 444*

(Received February 21, 1980)

Spin-state equilibria between a singlet low-spin and a triplet high-spin species of the title complexes in water were investigated by means of electronic spectra. The equilibrium constants and the thermodynamic parameters, ΔH and ΔS, were evaluated from detailed analysis of the temperature-dependence of the electronic spectra. The electronic spectra of the singlet and the triplet species involved were also derived, from the same analysis. The formation of the triplet species was found to be exothermic, which reflects the predominant contribution of the exothermic change to the formation of nickel(II)–water bond over the contribution of the endothermic change in the bond length caused by the change in spin state. The absolute values of ΔS almost correspond to those expected for the effective liberation of two molecules of water in aqueous solution.

Nickel(II) complexes with the title macrocyclic quadridentate ligands, $[\mathrm{Ni}(\mathrm{L}+n\mathrm{H})]^{2+}$ (n=−2 (**1**), 0 (**2**), 2 (**3**), and 4 (**4**): Fig. 1), have been reported to be often in an equilibrium between a singlet low-spin (diamagnetic square planar) and a triplet high-spin (paramagnetic pseudo octahedral) species in coordinating solvents,[1–3)] as described by

$$[\mathrm{Ni}(\mathrm{L}+n\mathrm{H})]^{2+} + 2\mathrm{S} \rightleftharpoons [\mathrm{Ni}(\mathrm{L}+n\mathrm{H})\mathrm{S}_2]^{2+}, \qquad (1)$$

where S denotes a coordinating solvent such as water, methanol, dimethyl sulfoxide, *N,N*-dimethylformamide, or acetonitrile.

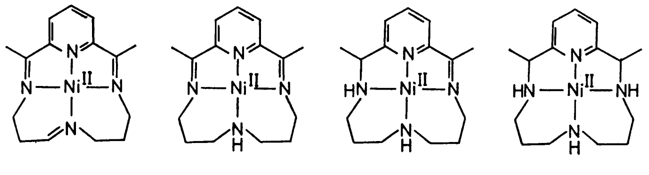

1 2 3 4

Fig. 1. Structural formulae of the complexes, $[\mathrm{Ni}(\mathrm{L}-2\mathrm{H})](\mathrm{ClO_4})_2$ (**1**), $[\mathrm{Ni}(\mathrm{L})](\mathrm{ClO_4})_2$ (**2**), $[\mathrm{Ni}(\mathrm{L}+2\mathrm{H})](\mathrm{ClO_4})_2$ (**3**), and $[\mathrm{Ni}(\mathrm{L}+4\mathrm{H})](\mathrm{ClO_4})_2$ (**4**).

Though the exact electronic spectra of the component species are required for the spectrophotometric evaluation of the equilibrium constant and the thermodynamic parameters for Equilibrium 1, evaluation of such component spectra was difficult because of the equilibrium immediately attained in a coordinating solvent.

In the present study we applied detailed analysis of the temperature-dependence of the electronic spectra to the spin-state equilibria of $[\mathrm{Ni}(\mathrm{L}+n\mathrm{H})]^{2+}$ in water for the evaluation of electronic spectra of the components, which allow the evaluation of equilibrium constants and thermodynamic parameters.

Experimental

Materials. Deionized water was distilled. Sodium perchlorate for the adjustment of ionic strength was recrystallized three times after traces of heavy metal ions had been removed. The nickel(II) complexes, $[\mathrm{Ni}(\mathrm{L}+n\mathrm{H})](\mathrm{ClO_4})_2$ (**1**—**4**), were synthesized according to the literature.[1,2,4,5)] The purity was confirmed by elemental analysis.

Measurements. The absorption spectra were measured with a Hitachi recording spectrophotometer model 340 equipped with a data printer, the absorbance being recorded within ±0.001. The temperature was measured with a copper-constantan thermocouple and a digital thermometer TAKEDA TR-2121, and maintained within ±0.1 °C. All measurements were carried out at a constant ionic strength, $I=0.1$ ($\mathrm{NaClO_4}$) (see below).

Analyses of the Data

Derivation of the electronic spectra of the component species and calculations of the equilibrium constants and the thermodynamic parameters were carried out as follows, an appropriate computer program being designed for the present purpose.[6)]

The equilibrium constant for Eq. 1 is defined as

$$K = [\text{triplet}]/[\text{singlet}]. \qquad (2)$$

This equation is transformed into Eq. 3 by introducing the molar absorption coefficients at an arbitrary wavelength λ_n, ε_{sn} and ε_{tn}, for the singlet and the triplet species, respectively, and the apparent molar absorption coefficient, $\varepsilon_{\mathrm{obs}n}$, for the solution in equilibrium,

$$K = (\varepsilon_{sn}-\varepsilon_{\mathrm{obs}n})/(\varepsilon_{\mathrm{obs}n}-\varepsilon_{tn}). \qquad (3)$$

At the wavelength λ_0 where ε_{s0} equals 0, Eq. 3 becomes

$$K = \frac{\varepsilon_{\mathrm{obs}0}}{\varepsilon_{t0}-\varepsilon_{\mathrm{obs}0}}. \qquad (4)$$

The temperature-dependence of the equilibrium constant, K, is given by Eq. 5, provided that the molar absorption coefficients for the singlet and the triplet species do not depend on the temperature

$$\ln K = \ln\left(\frac{\varepsilon_{\mathrm{obs}0}}{\varepsilon_{t0}-\varepsilon_{\mathrm{obs}0}}\right) = \frac{\Delta S_0}{R} - \frac{\Delta H_0}{RT}. \qquad (5)$$

Since Eq. 3 also holds at an arbitrary wavelengh λ_n, the following relationship is immediately derived:

$$\varepsilon_{\mathrm{obs}n} = \varepsilon_{sn} - \frac{(\varepsilon_{sn}-\varepsilon_{tn})}{\varepsilon_{t0}}\cdot\varepsilon_{\mathrm{obs}0}, \qquad (6)$$

where $\varepsilon_{\mathrm{obs}n}$ and $\varepsilon_{\mathrm{obs}0}$ denote the apparent molar absorption coefficients at T K observed at λ_n and λ_0, respectively. This equation enables the calculation of the absorption coefficients, ε_{sn} and ε_{tn}, at any arbitrary wavelength λ_n from the plot of $\varepsilon_{\mathrm{obs}n}$ against $\varepsilon_{\mathrm{obs}0}$ at various temperatures. The absorption spectra for the singlet and the triplet form are constructed by plotting the values of $\varepsilon_{\mathrm{s}n}$ and $\varepsilon_{\mathrm{t}n}$ against the wavelengths λ_n, respectively.

The Arrhenius equation holds also in terms of $\varepsilon_{\mathrm{s}n}$ and $\varepsilon_{\mathrm{obs}n}$:

$$\ln K = \ln\left(\frac{\varepsilon_{\mathrm{s}n}-\varepsilon_{\mathrm{obs}n}}{\varepsilon_{\mathrm{obs}n}-\varepsilon_{\mathrm{t}n}}\right) = \frac{\Delta S_n}{R} - \frac{\Delta H_n}{RT}. \quad (7)$$

The thermodynamic parameters, ΔS_n and ΔH_n, are evaluated from Eq. 7. The values of molar absorption coefficient at λ_n could be calculated by Eq. 8 with respect to K,

$$\varepsilon_{\mathrm{calc}n} = \varepsilon_{\mathrm{s}n} + \frac{\varepsilon_{\mathrm{s}n}-\varepsilon_{\mathrm{t}n}}{1+K}. \quad (8)$$

Actual calculations were carried out according to the following directions by means of an appropriate computer program which includes the least-square fits for Eqs. 5 and 7.[6)]

(1) Choose the wavelength λ_0 where $\varepsilon_{\mathrm{s}0}=0$ (In some cases λ_0 where $\varepsilon_{\mathrm{t}0}=0$ should be chosen).

(2) Calculate the value of K at T K by means of Eq. 4 for an appropriate value of $\varepsilon_{\mathrm{t}0}$ and plot the value of log K against T^{-1} by means of Eq. 5.

(3) Repeat the calculations in (2) by changing the values of $\varepsilon_{\mathrm{t}0}$ until a linear plot is obtained. Determine the optimum value for $\varepsilon_{\mathrm{t}0}$.

(4) For the optimum value of $\varepsilon_{\mathrm{t}0}$ evaluated in (3), plot the values of $\varepsilon_{\mathrm{obs}n}$ against those of $\varepsilon_{\mathrm{obs}0}$ at various temperatures by means of Eq. 6. Evaluate the values of $\varepsilon_{\mathrm{s}n}$ and $\varepsilon_{\mathrm{t}n}$ at λ_n from the slope $(\varepsilon_{\mathrm{s}n}-\varepsilon_{\mathrm{t}n})/\varepsilon_{\mathrm{t}0}$ and the intercept $\varepsilon_{\mathrm{s}n}$.

(5) Calculate the value of K_n at T K with the values of $\varepsilon_{\mathrm{s}n}$ and $\varepsilon_{\mathrm{t}n}$ by means of Eq. 7 and plot the Arrhenius relationship. Evaluate the values of ΔH_n and ΔS_n at λ_n from the slope and the intercept. Confirm the coincidence of all values with each other for ΔH_n and ΔS_n obtained at λ_n.

(6) Calculate the values of $\varepsilon_{\mathrm{calc}n}$ at various λ_n with the values of K, ΔH and ΔS, and $\varepsilon_{\mathrm{s}n}$ and $\varepsilon_{\mathrm{t}n}$. Confirm the coincidence of the calculated values of $\varepsilon_{\mathrm{calc}n}$ with those of $\varepsilon_{\mathrm{obs}n}$ measured at λ_n.

Results and Discussion

Figure 2 shows the electronic spectra of $[\mathrm{Ni(L)}]^{2+}$ in water at various temperatures. The spectrum changes reversibly with an isosbestic point at 590 nm. With rise in temperature the absorption at 395 nm remarkably increases and the absorption at 720 nm decreases. Based on the assignment of the absorption maxima at 450 and 720 nm to the singlet and the triplet species, respectively, we deduced that the given spectral change corresponds to the temperature-dependence of the spin-state equilibrium of the given complex between the singlet square planar and the triplet pseudo octahedral species. Similar temperature-dependence in the electronic spectra was observed also for the other analogous $[\mathrm{Ni(L}+n\mathrm{H)}]^{2+}$–$\mathrm{H_2O}$ systems, indicating the temperature-dependent equilibrium between the triplet and the singlet species.

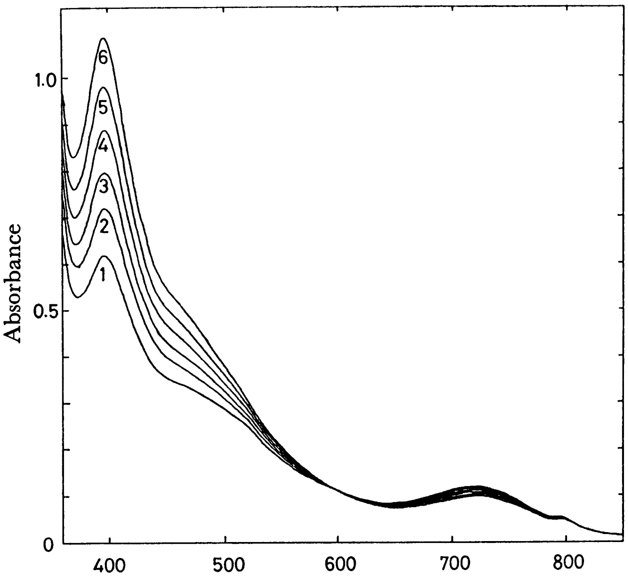

Fig. 2. Absorption spectra of $[\mathrm{Ni(L)}](\mathrm{ClO_4})_2$ in $\mathrm{H_2O}$ (4.98×10^{-3} mol dm^{-3}) at various temperatures. At I=0.1 ($\mathrm{NaClO_4}$). Measured at 279.2 (1), 285.6 (2), 290.0 (3), 294.8 (4), 299.3 (5), and 303.8 K (6).

The detailed analyses of the temperature-dependence of the spectra as described in the foregoing section allowed us to calculate the equilibrium constant, K, and the thermodynamic parameters, ΔH and ΔS, of Equilibrium 1 and also to derive the individual spectrum of the singlet and the triplet species. Since in the $[\mathrm{Ni(L)}]^{2+}$–$\mathrm{H_2O}$ system an absorption peak at 720 nm assigned to a triplet species is well separated from the absorption peaks of the singlet species appearing at shorter wavelengths, 720 nm was adopted as an appropriate wavelength λ_0 for the $[\mathrm{Ni(L)}]^{2+}$–$\mathrm{H_2O}$ system, where $\varepsilon_{\mathrm{s}0}=0$.

Figure 3 shows a set of plots of log K for the $[\mathrm{Ni(L)}]^{2+}$–$\mathrm{H_2O}$ system against T^{-1} as derived from Eq. 5 for various values of $\varepsilon_{\mathrm{t}0}$. We see that only the plot for $\varepsilon_{\mathrm{t}0}=27.6$ mol^{-1} dm^3 cm^{-1} gives a straight line; for any values of $\varepsilon_{\mathrm{t}0}$ larger than 27.6 mol^{-1} dm^3 cm^{-1} the plot always gives a curve with positive curvature, and for any values of $\varepsilon_{\mathrm{t}0}$ smaller than 27.6 mol^{-1} dm^3 cm^{-1} a curve with negative curvature. The values of $\varepsilon_{\mathrm{s}n}$ and $\varepsilon_{\mathrm{t}n}$ at an arbitrary wavelength λ_n are evaluated using this value of $\varepsilon_{\mathrm{t}0}$ and the values of $\varepsilon_{\mathrm{obs}n}$ by means of Eq. 6. The validity of the value 27.6 mol^{-1} dm^3 cm^{-1} as $\varepsilon_{\mathrm{t}0}$ was again confirmed for the linear dependence on T^{-1} of the values of K derived from the values of $\varepsilon_{\mathrm{s}n}$ and $\varepsilon_{\mathrm{t}n}$ using Eq. 7. The values of ΔH and ΔS were calculated as slopes and intercepts by means of Eqs. 5 and 7. The adopted wavelength λ_0 and the evaluated $\varepsilon_{\mathrm{t}0}$ for the series of $[\mathrm{Ni(L}+n\mathrm{H)}]^{2+}$–$\mathrm{H_2O}$ systems are summarized in Table 1.

Figure 4(a) shows the electronic spectra of the singlet and the triplet species, $[\mathrm{Ni(L)}]^{2+}$ and $[\mathrm{Ni(L)(OH_2)_2}]^{2+}$, reproduced by plotting against λ_n the values of $\varepsilon_{\mathrm{s}n}$ and $\varepsilon_{\mathrm{t}n}$ calculated by means of Eq. 6, respectively. The absorption maximum at 395 nm (ε=1011 mol^{-1}

dm^3 cm^{-1}) and the d-d absorption band around 450 nm are clearly shown in the spectrum of the singlet species. A remarkable feature in the electronic spectrum of the triplet species is the clear discrimination of a weak absorption band around 520 nm by the analysis of electronic spectra. The band is almost included in the envelope of a very strong singlet band and is observed only as an indiscernibly weak shoulder in Fig. 2. Figure 4(b) shows the electronic spectra of the singlet and the triplet species in the *meso*-[Ni$(\mathrm{L+4H})]^{2+}$–H_2O system. The weak absorption band around 500 nm of the triplet species, not recognized in the spectrum of the equilibrium mixture of the triplet and the singlet species, is also clearly discriminated by the same analysis. The results indicate that the proposed analysis is useful also for the de-

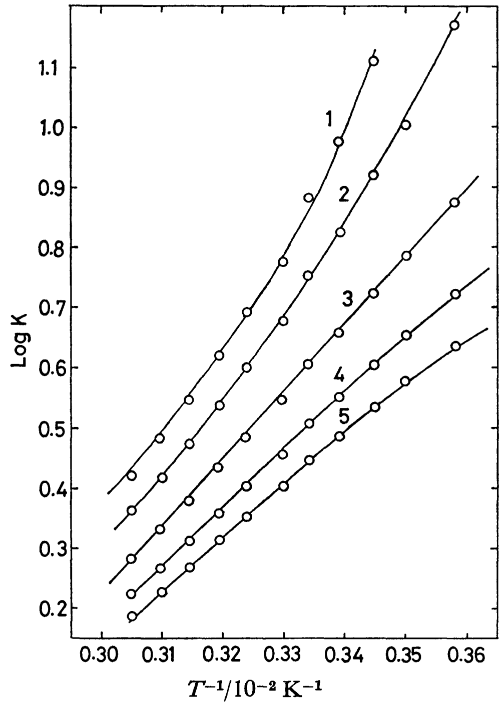

Fig. 3. Plots of log *K* *vs.* T^{-1} for [Ni(L)]$(\mathrm{ClO_4})_2$ (4.98×10^{-3} mol dm^{-3}) for various values of ε_{t0} at 720 nm. The values of ε_{t0} at 720 nm: 25.0 (1), 26.0 (2), 27.6 (3), 29.0 (4), and 30.0 mol^{-1} dm^3 cm^{-1} (5).

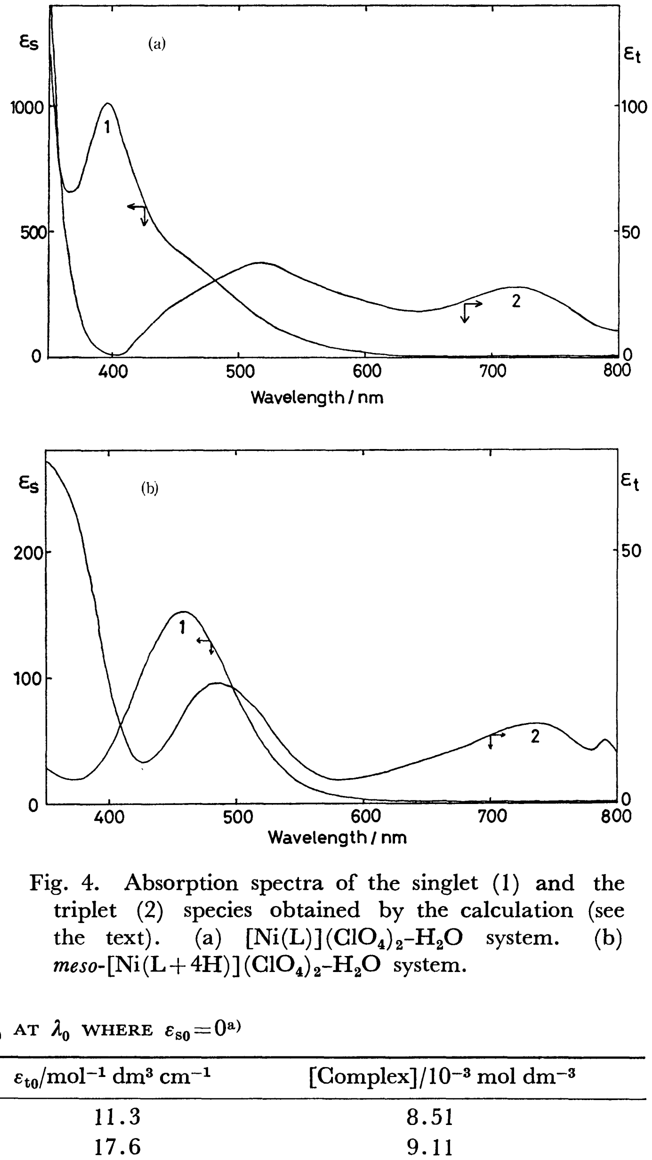

Fig. 4. Absorption spectra of the singlet (1) and the triplet (2) species obtained by the calculation (see the text). (a) [Ni(L)]$(\mathrm{ClO_4})_2$–H_2O system. (b) *meso*-[Ni(L+4H)]$(\mathrm{ClO_4})_2$–H_2O system.

Table 1. Evaluated ε_{t0} at λ_0 where $\varepsilon_{s0}=0^{\mathrm{a)}}$

	λ_0/nm	ε_{t0}/mol^{-1} dm^3 cm^{-1}	[Complex]/10^{-3} mol dm^{-3}
meso-[Ni(L+4H)[$(\mathrm{ClO_4})_2{}^{\mathrm{b)}}$	735	11.3	8.51
rac-[Ni(L+4H)]$(\mathrm{ClO_4})_2{}^{\mathrm{c)}}$	730	17.6	9.11
[Ni(L+2H)]$(\mathrm{ClO_4})_2$	725	22.4	8.07
[Ni(L)]$(\mathrm{ClO_4})_2$	720	27.6	4.98
[Ni(L−2H)]$(\mathrm{ClO_4})_2$	720	8.2	4.36

a) At $I=0.1$ (NaClO$_4$). b) *α-C-meso* isomer (see Ref. 5). c) *C-rac* isomer.

Table 2. Equilibrium constants in $H_2O^{\mathrm{a)}}$

	K	*T*/K	*K*	*T*/K
meso-[Ni(L+4H)]$(\mathrm{ClO_4})_2{}^{\mathrm{b)}}$	0.31_2	299.4	0.28_0	303.5
rac-[Ni(L+4H)]$(\mathrm{ClO_4})_2{}^{\mathrm{c)}}$	0.45_9	299.4	0.41_2	303.4
[Ni(L+2H)]$(\mathrm{ClO_4})_2$	0.55_6	299.3	0.49_4	303.5
[Ni(L)]$(\mathrm{ClO_4})_2$	3.99_6	299.3	3.59_5	303.0
[Ni(L−2H)]$(\mathrm{ClO_4})_2$	0.59_3	299.3	0.51_9	303.8

a) Under the same conditions as in Table 1. *K*=[triplet]/[singlet]. b) *α-C-meso* isomer (see Ref. 5). c) *C-rac* isomer.

tection of unknown weak absorption bands of the components hidden in the spectrum of an equilibrium mixture.

The values of equilibrium constants, K, at 299.3 ± 0.1 and 303.4 ± 0.4 K are given in Table 2. The value of K at 299.3 K is larger than that at 303.4 K, indicating a decrease in the triplet form with rise in temperature. The degree of formation of the triplet species for $[Ni(L)](ClO_4)_2$ is the largest among the given $[Ni(L+nH)](ClO_4)_2$–H_2O systems. This can be interpreted as follows. The in-plane ligand-field strength is assumed to be in the order, $[Ni(L+4H)]^{2+} < [Ni(L+2H)]^{2+} < [Ni(L)]^{2+} < [Ni(L-2H)]^{2+}$.[7] On the other hand, the steric hindrance at an axial coordination site caused by the proton of secondary amine and/or methyl moiety in the ligand molecule is assumed to be in the reversed order. The ease with which an axial ligand coordinates to the central atom is expected to be the largest at $[Ni(L)]^{2+}$ having moderate effects both in the in-plane ligand-field strength and in the steric hindrance at an axial coordination site.

The thermodynamic parameters for Equilibrium 1 are given in Table 3 (see Experimental). The negative values of ΔH indicate that formation of the triplet species is exothermic for all $[Ni(L+nH)]^{2+}$–H_2O systems. For the complexes of similar quadridentate ligands the Ni–N bond length has been reported to be $(2.07–2.10) \times 10^{-8}$ cm in the high-spin complexes and $(1.88–1.91) \times 10^{-8}$ cm in the singlet low-spin complexes.[7,8] For the formation of a triplet species the Ni–N bonds in a complex should be elongated; this change in the bond length in the in-plane ligand should cause the endothermic effects. The negative values of ΔH obtained reflect the exothermic contribution of the formation of Ni–water bond exceeding the endothermic contribution of change in the spin-state.

Table 3. Thermodynamic parameters[a)]

	$-\Delta H$ 10^4 J mol^{-1}	$-\Delta S$ J K^{-1} mol^{-1}
meso-$[Ni(L+4H)](ClO_4)_2$[b)]	2.02	77.0
rac-$[Ni(L+4H)](ClO_4)_2$[c)]	2.04	74.9
$[Ni(L+2H)](ClO_4)_2$	2.16	77.0
$[Ni(L)](ClO_4)_2$	2.12	59.4
$[Ni(L-2H)](ClO_4)_2$	2.32	82.0

a) Under the same conditions as in Table 1. b) α-*C-meso* isomer (see Ref. 5). c) *C-rac* isomer.

The absolute values of ΔS nearly correspond to those expected for the effective liberation of two water molecules from the title complexes in aqueous solution, *viz.*, $(30\sim40) \times 2$ J K^{-1} mol^{-1}.[9]

Table 4. Effect of $NaClO_4$ on the equilibrium constants[a)]

$[Ni(L)](ClO_4)_2$[b)]		*rac*-$[Ni(L+4H)](ClO_4)_2$[c)]	
$\frac{[NaClO_4]}{\text{mol dm}^{-3}}$	K	$\frac{[NaClO_4]}{\text{mol dm}^{-3}}$	K
0	6.87	0	0.623
0.040	4.83	0.040	0.479
0.080	4.21	0.080	0.422
0.161	3.41	0.200	0.323
0.282	2.66	0.400	0.229
0.402	2.17	0.800	0.144
0.805	1.21	1.200	0.082
1.207	0.75	1.552	0.051

a) $K = \frac{[\text{triplet}]}{[\text{singlet}]}$. b) 3.98×10^{-3} mol dm^{-3} at $T = 298.8$ K. c) 2.65×10^{-3} mol dm^{-3} at $T = 299.2$ K. *C-rac* isomer.

Table 4 shows the effects of the addition of $NaClO_4$ on the spin-state equilibria in the $[Ni(L)]^{2+}$– and the *rac*-$[Ni(L+4H)]^{2+}$–H_2O system. In both cases addition of $NaClO_4$ enhanced the intensity of the singlet bands, which shows the increase in the singlet species in equilibrium. In a solution containing high concentrations of $NaClO_4$, *e.g.*, 6 mol dm^{-3}, no temperature-dependence of the spectrum was observed, showing the predominance of the singlet species in the equilibrium. The value of molar absorption coefficient ($\varepsilon = 1167$ mol^{-1} dm^3 cm^{-1}) measured in 6 mol dm^{-3} $NaClO_4$ at 395 nm, absorption maximum for the singlet species, agreed with that evaluated from the above calculation. The decrease in K with increasing concentrations of $NaClO_4$ was almost the same in the case of the $[Ni(L)]^{2+}$– and the *rac*-$[Ni(L+4H)]^{2+}$–H_2O system. A similar effect has been reported in other spin-state equilibria such as $[Ni(trien)]^{2+}$–H_2O,[10] $[Ni(cyclam)]^{2+}$–H_2O,[11] and $[Ni(isocyclam)]^{2+}$–H_2O systems,[12] where trien, cyclam, and isocyclam denote quadridentate ligands, triethylenetetramine, 1,4,8,11-tetraazacyclotetradecane, and 1,4,-7,11-tetraazacyclotetradecane, respectively. On the basis of these observations, all measurements in the preceding paragraphs were carried out at a constant ionic strength, $I = 0.1$ ($NaClO_4$).

Calculations were carried out on the HITAC M-200H computer at the Computer Center, Institute for Molecular Science and on the FACOM M230-60 computer at Hokkaido University Computing Center. This work was supported by the Joint Studies Program (1978—1979) of the Institute for Molecular Science.

References

1) J. L. Karn, Ph.D. Dissertation, The Ohio State University, 1966; J. L. Karn and D. H. Busch, *Inorg. Chem.*, **8**, 1149 (1969).

2) E. K. Barefield, F. V. Lovecchio, N. E. Tokel, E. Ochiai, and D. H. Busch, *Inorg. Chem.*, **11**, 283 (1972).

3) L. Runsnak and R. B. Jordan, *Inorg. Chem.*, **10**, 2199 (1971).

4) K. Mochizuki, T. Ito, and M. Fujimoto, *Bull. Chem. Soc. Jpn.*, **53**, 543 (1980).

5) E. Ochiai and D. H. Busch, *Inorg. Chem.*, **8**, 1798 (1969).

6) The further details and improvement of this method will be reported elsewhere. T. Ito, H. Ito, J. Suzuki, and J. Fujita, unpublished study. Refer to T. Ito for the computer program for calculations.

[7] For the detailed discussion, see L. Y. Martin, D. R. Seperati, and D. H. Busch, *J. Am. Chem. Soc.*, **99**, 2968 (1977).

[8] P. O. Whimp, M. F. Bailey, and N. F. Curtis, *J. Chem. Soc., A*, **1970**, 1956; L. N. Swink and M. Atoji, *Acta Crystallogr.*, **13**, 639 (1960); J. M. Waters and K. R. Whittle, *J. Inorg. Nucl. Chem.*, **34**, 155 (1972); T. Ito and K. Toriumi, *Chem. Lett.*, **1978**, 1395.

[9] F. P. Hinz and D. W. Margerum, *Inorg. Chem.*, **13**, 294 (1974).

[10] C. K. Jørgensen, *Acta Chem. Scand.*, **11**, 399 (1957).

[11] A. Anichini, L. Fabbrizzi, and P. Paoletti, *Inorg. Chim. Acta*, **24**, L21 (1977).

[12] L. Sabatini and L. Fabbrizzi, *Inorg. Chem.*, **18**, 438 (1979).